PHYSICAL REVIEW E **69**, 035403(R) (2004)

Control of laser-beam propagation and absorption in a nanoplasma gas by programming of a transient complex refractive index with a prepulse

H.-H. Chu,[1,2] H.-E. Tsai,[1,3] Y.-F. Xiao,[1,2] C.-H. Lee,[4] J.-Y. Lin,[5] J. Wang,[1,3,6] and S.-Y. Chen[1]

[1]*Institute of Atomic and Molecular Sciences, Academia Sinica, Taipei 106, Taiwan*

[2]*Department of Physics, National Taiwan University, Taipei 106, Taiwan*

[3]*Graduate Institute of Electro-Optical Engineering, National Taiwan University, Taipei 106, Taiwan*

[4]*Institute of Applied Science and Engineering Research, Academia Sinica, Taipei 115, Taiwan*

[5]*Department of Physics, National Chung Cheng University, Chia-Yi 621, Taiwan*

[6]*Department of Electrical Engineering, National Taiwan University, Taipei 106, Taiwan*

(Received 7 October 2003; published 31 March 2004; publisher error corrected 23 April 2004)

By utilizing the intensity- and duration-dependent heating and expansion rate of nanoplasma to generate a transient transverse gradient of the refractive index, prepulse controlled laser-beam propagation is demonstrated. The dynamical response of the macroscopic optical refractive index is traced back to the microscopic polarizability of nanoplasmas experimentally, in accordance with hydrodynamic nanoplasma models. In particular, the delay between the prepulse and the main pulse for maximum Rayleigh scattering is found to be longer than that for maximum x-ray emission, supporting the more refined one-dimensional self-consistent hydrodynamic nanoplasma model.

DOI: 10.1103/PhysRevE.69.035403 PACS number(s): 52.38.Hb, 36.40.Vz, 36.40.Gk

With the rapid progress in high-power laser technology in the past decade, the interaction of ultrashort high-intensity laser pulses with atomic clusters has become an active field of research. As a result of their solidlike local density and gaslike average density, it has been shown that individual nanometer clusters can absorb laser energy efficiently to form highly charged hot nanoplasmas [1,2], eject keV electrons [3] and MeV ions [4], and emit strongly from extreme ultraviolet to hard x ray [5,6]. Nuclear fusion have also been demonstrated by collisions of high-energy ions produced from laser-heated deuterium clusters [7]. Various models have been constructed to help understand this complex process.

In the hydrodynamic nanoplasma model used in Ref. [8], it is assumed that a laser-heated nanoplasma expands with uniform density and temperature. The model explains several key features of the experiments qualitatively, such as high degree ionization, generation of energetic electrons and ions, strong x-ray emission, and resonant laser-cluster coupling at an optimal pulse duration [9,10]. A self-consistent one-dimensional (1D) model that removes the constraint of uniform density and temperature is used in Ref. [11], which leads to a better quantitative estimation of the optimal pulse duration and the nanoplasma polarizability [12]. Recently, a two-dimensional hydrodynamic model was used to explain the observations of asymmetric ion ejection from laser-heated clusters [13]. In addition to these models, particle-dynamics simulations have been used to study the laser-cluster interaction [14–16]. These simulations are limited to small clusters, but provide a better prediction of the expansion dynamics and electron/ion spectrum.

Given the microscopic pictures, the macroscopic optical properties of a bulk nanoplasma gas were derived in Ref. [17] following the uniform density model. It is shown that as the intrananoplasma electron density varies from supercritical to subcritical, the real part of the nanoplasma polarizability varies from $\gamma_{\mathrm{real}}>0$ to $\gamma_{\mathrm{real}}<0$, leading to the change of the refractive index of the bulk nanoplasma gas from $n>1$ to $n<1$. When a nanoplasma is heated by a laser pulse, the intrananoplasma electron density first rises to a supercritical level due to collisional ionization and subsequently decreases to a subcritical level as a result of nanoplasma expansion, resulting in the transient change of the bulk refractive index from $n\approx 1$ to $n>1$ and then down to $n<1$. This has been observed in Ref. [12], which also verified the relation between the real part (refractive index) and the imaginary part (absorption) of the transient ensemble-averaged polarizability. In Ref. [18] it was reported that a laser pulse with suitable pulse duration can weakly self-focus as it propagates in a bulk nanoplasma gas. This was attributed to the effect of the transverse laser intensity distribution. When a laser beam is focused into a bulk nanoplasma gas, the on-axis nanoplasmas are heated more rapidly than those at the outer region, so the on-axis refractive index rises and then falls faster compared to that of the outer region. This leads to a convex radial profile of refractive index in the beginning and a concave radial profile afterwards, acting effectively as a transient lens with a focal length changing from positive to negative with time.

In this paper, we demonstrate the control of laser pulse propagation in a bulk nanoplasma gas by using a prepulse to modify the transient refractive index. The microscopic absorption and expansion dynamics are also studied with pump-probe Rayleigh scattering [19] and soft x-ray fluorescence. The time-varying beam convergence provides direct evidences of the relation between macroscopic optical properties of the nanoplasma gas and its microscopic polarizability. In particular, we find that the optimal delay between the prepulse and the main pulse for maximum Rayleigh scattering is longer than that for maximum x-ray emission. The separation of the peaks of absorption and scattering verifies the prediction of 1D self-consistent hydrodynamic nanoplasma model.

A 10 TW, 55 fs, 810 nm, 10 Hz Ti:sapphire laser system based on chirped-pulse amplification was used for our experiment. The laser contrast is $>10^8$ at -10 ns, $>10^6$ at -50 ps, and $>10^4$ at -1 ps. After the final-stage amplifier, the laser beam is expanded to 40 mm in clear aperture. The beam is then split into two, each part going through an energy tuner and a pulse compressor. With this double compressor configuration, the pulse duration, chirp, energy, beam size, and delay of these two laser beams can be controlled independently with a combined maximal energy of 550 mJ. After being recombined by using a thin-film polarizer and a half-wave plate, the two beams copropagate and are focused with an off-axis parabolic mirror onto an argon gas jet. The focal spot of the main pulse fits well to a Gaussian profile of 8.5 μm full width at half maximum (FWHM), with 80% energy enclosed, and the focal spot of the prepulse is enlarged to 18 μm FWHM by inserting a 2 cm diameter hard aperture in the path of the prepulse before recombination. The gas jet is produced with a pulsed valve and a supersonic nozzle, having a flat-top region of 1 mm in length and a sharp boundary of 250 μm at both edges [20]. Clusters are formed inside this jet as a result of rapid adiabatic cooling. From Hagena's formula [21], the average cluster size is estimated to be 10–60 nm for a backing pressure of 100–800 psi with our nozzle geometry. Side imaging of Rayleigh scattering from nanoplasmas, bandpass filtered at 810 nm, is used to observe the propagation of laser beam in the bulk nanoplasma gas, and to measure the spatially resolved temporal evolution of the magnitude of nanoplasma polarizability. Mach-Zehnder interferometry with a 10% probe beam split from the main beam passing transversely through the gas jet is used to observe the *spatially and temporally resolved* propagation of the prepulse and main pulse [20]. In addition, a relay-imaging system is used to measure the beam profile at the exit plane of the clustered gas jet [20], in which a linear polarizer is put in front of the charge-coupled device camera to block the image of the prepulse and thus only the main-pulse profile is recorded. A calibrated x-ray *p-i-n* diode detector equipped with a 3 μm Be filter is used to measure the integrated x-ray yield from 11 to 14 nm in the transverse direction.

The magnitude of the nanoplasma polarizability $|\gamma|$ can be measured by imaging the Rayleigh scattering of the laser pulse in the direction perpendicular to laser propagation [12]. In this experiment, a prepulse is used to preionize clusters to form nanoplasmas and at the same time heat up the nanoplasmas to drive their expansion. A main pulse following the prepulse at proper timing interacts with the preformed nanoplasmas. According to the hydrodynamic nanoplasma model, the magnitude of nanoplasma polarizability $|\gamma|$ reaches a maximum when the intrananoplasma electron density drops from a solidlike density to the resonant density. Therefore an optimal main-pulse delay for strongest Rayleigh scattering is expected. Fig. 1(a) shows the Rayleigh scattering images at three different main-pulse delays. The polarizations of the two pulses are linear and oriented such that only the Rayleigh scattering of the main pulse is collected. When the delay increases, the bright region moves downstream. By dividing the images into five sections and integrating the signal in each section, it is observed that the optimal delay for strongest scattering is longer for positions further downstream, as shown in Fig. 1(b). When the prepulse propagates through the argon cluster jet, its intensity decreases gradually due to absorption by the ionized clusters. As a result, the initial temperature of the nanoplasmas generated by the prepulse is lower toward the exit plane, so the expansion speed is smaller and the optimal delay is longer. This result verifies that the side-scattering images are indeed the Rayleigh-scattering images of the nanoplasmas, and the spatially resolved temporal evolution of the magnitude of nanoplasma polarizability can be measured with this method.

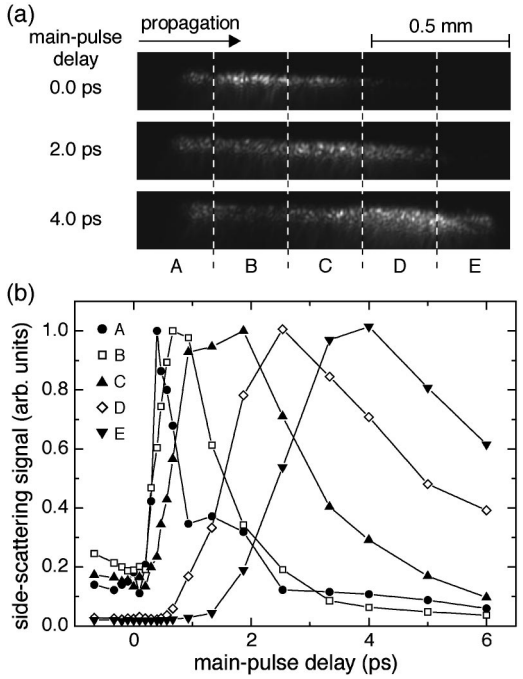

FIG. 1. Side images of Rayleigh scattering (a) and integrated scattering signal in each section (b) as a function of main-pulse delay. Prepulse: 2.0 mJ, 70 fs. Main pulse: 11 mJ, 70 fs. Backing pressure: 300 psi.

In this experiment, the main pulse propagation in the Ar nanoplasma gas is controlled by programming the prepulse intensity, duration, and relative delay. The prepulse is stretched to 540 fs for optimal nanoplasma-induced self-focusing. This slightly self-focused prepulse can preserve its beam size and intensity for longer distance and thus maintain a near uniform transient lens along the path. The result is shown in Fig. 2(a) with various main-pulse delays. With zero delay, the beam refocuses slightly and then slowly diverges. As the delay is increased to 1 ps, the beam refocuses strongly and then diverges quickly. When the delay is further increased, the beam diverges without refocusing. The corresponding spatial profiles of the main pulse at the exit edge of the clustered gas jet are shown in Fig. 2(b). The results are consistent with Fig. 2(a). The beam diameter of the main pulse and the integrated Rayleigh scattering signal as functions of delay are shown in Fig. 3. The increase of Rayleigh scattering and the decrease of beam diameter are strongly correlated, verifying the direct link between the microscopic

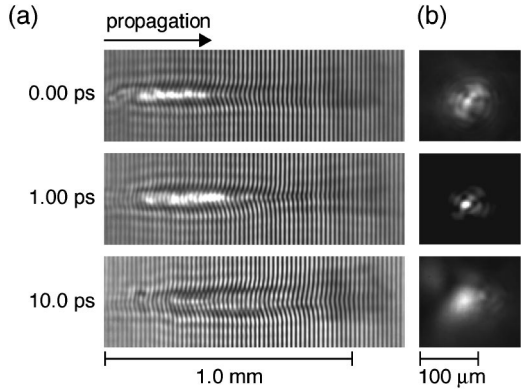

FIG. 2. Interferograms (a) and beam profile images of the main pulse at the exit plane (b) as a function of main-pulse delay. Prepulse: 2.2 mJ, 540 fs. Main pulse: 11 mJ, 55 fs. Backing pressure: 500 psi.

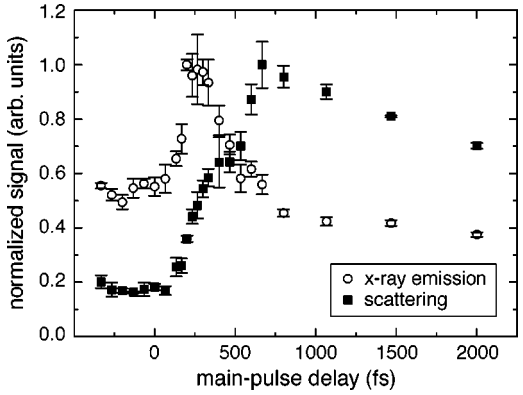

FIG. 4. X-ray yield in the 11–14 nm wavelength range (open circle) and integrated Rayleigh-scattering signal (solid square) from the main pulse as a function of main-pulse delay. Prepulse: 10 mJ, 70 fs. Main pulse: 40 mJ, 70 fs. Backing pressure: 500 psi.

nanoplasma polarizability and the macroscopic refractive index of the bulk nanoplasma gas.

The beam diameter of the main pulse as a function of delay for different cluster sizes is also measured by varying the backing pressure. The inset of Fig. 3 shows the main-pulse delay for minimum beam diameter is deferred from 1 to 2 ps when the backing pressure is increased from 500 to 800 psi, corresponding to a change of the cluster size from 40 nm to 60 nm. This agrees with the fact that nanoplasmas of larger clusters take more time to expand from supercritical to subcritical density. As a null test we also do the same measurement with a He gas jet for which no cluster can be formed under the same experimental conditions. In contrast to the results of the Ar cluster jet, the main-pulse diameter shows only a mild monotonic increase with main-pulse delay. This identifies that the focusing and defocusing effect in the Ar cluster jet are indeed from the transient polarizability of nanoplasmas created by the prepulse.

As the electrons in nanoplasmas oscillate under the driving force of the laser field, the collisions between electrons

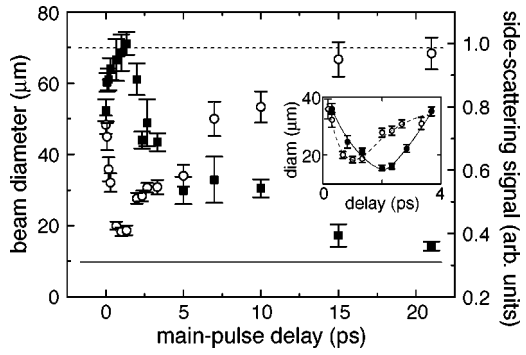

FIG. 3. Diameter of the main pulse at the exit plane of the cluster jet (open circle) and integrated Rayleigh-scattering signal (solid square) of the main pulse as a function of main-pulse delay under the same experimental condition as in Fig. 2. The dashed and solid lines represent the case without a prepulse to preionize Ar clusters. Inset shows the main-pulse diameter at the exit plane as a function of main-pulse delay for a backing pressure of 500 psi (open circle) and 800 psi (solid circle).

and ions lead to heating of the electrons, which in turn results in collisional excitation and ionization of ions and thus emission of x rays. It was shown experimentally that the x-ray yield of the nanoplasmas remained proportional to the absorbed laser energy as the pulse duration of the driving laser was varied [9]. The uniform-density nanoplasma model predicts that when the nanoplasma oscillation amplitude $|\gamma|$ reaches maximum, the absorption γ_{imag} should also be at maximum [8,22]. Therefore the optimal pulse duration for maximum scattering and absorption should be the same. However, this does not agree with the observations in Ref. [22], which shows that the optimal pulse duration for maximum Rayleigh scattering is larger than that for maximum absorption. On the other hand, in the 1D self-consistent hydrodynamic model [11,12] γ_{imag} is proportional to the volume of the critical density shell and γ_{real} is determined by the competition between the supercritical density shell (contributing a positive γ_{real}) and the subcritical density shell (contributing a negative γ_{real}). This leads to γ_{real} crossing zero occurs earlier than γ_{imag} reaching a maximum during the expansion process according to the simulation in Ref. [12]. Therefore, $|\gamma|$ should reach a maximum later than γ_{imag}, resulting in the delay of maximum Rayleigh scattering. To verify this, we measured Rayleigh scattering and x-ray yield simultaneously as functions of the main-pulse delay. The duration of the prepulse is chosen to be 70 fs such that the propagation of the main pulse is not affected by the prepulse when the main-pulse delay is varied. The x-ray yield from the main pulse which corresponds to the absorption is obtained by subtracting the small yield measured without the main pulse. The whole Rayleigh scattering image of the main pulse is integrated in order to be compared with the spatially integrated x-ray yield. As shown in Fig. 4, the optimal delay for maximum x-ray emission is 300 fs and that for Rayleigh scattering is 700 fs. This result strongly supports the 1D self-consistent hydrodynamic model rather than the uniform density model. In addition, the Rayleigh scattering falls much slower with increasing delay after the peak than the x-ray signal does. This agrees with the common description of the uniform density model and the 1D self-consistent model that as the nanoplasmas expand continuously γ_{imag}

should converge to zero and γ_{real} to that of uniform plasma.

We have demonstrated optically controlled focusing by manipulating the transient spatial profile of nanoplasma polarizability with a prepulse. Corresponding variations in the microscopic polarizability and macroscopic optical refractive index are observed in accordance with the hydrodynamic nanoplasma model. The main-pulse delay for maximum Rayleigh scattering is found to be longer than that for maximum x-ray emission. This is a new evidence to support the 1D self-consistent hydrodynamic nanoplasma model in comparison with the uniform density model. By simultaneously measuring the microscopic and macroscopic effects of the transient polarizability, this work provides a direct check of the hydrodynamic nanoplasma model. In perspective, the unique properties of nanoplasma gas could contribute to the research of plasma nonlinear optics such as phase matching of high-order harmonic generation [17,23]. The control of nanoplasma heating and laser beam propagation in a clustered gas jet simultaneously by using a prepulse has produced an efficient incoherent x-ray source (12% conversion efficiency in the 11–20 nm range), and may also lead to the development of new schemes of transient collisional x-ray lasers.

This work was partly supported by the National Science Council of Taiwan under the Grant No. NSC 92-2112-M-194.

[1] T. Ditmire, R.A. Smith, J.W.G. Tisch, and M.H.R. Hutchinson, Phys. Rev. Lett. **78**, 3121 (1997).
[2] M.M. Murnane *et al.*, Appl. Phys. Lett. **62**, 1068 (1993).
[3] Y.L. Shao *et al.*, Phys. Rev. Lett. **77**, 3343 (1996).
[4] T. Ditmire *et al.*, Nature (London) **386**, 54 (1997).
[5] A. McPherson *et al.*, Nature (London) **370**, 631 (1994).
[6] S. Dobosz *et al.*, Phys. Rev. A **56**, R2526 (1997).
[7] T. Ditmire *et al.*, Nature (London) **398**, 489 (1999).
[8] T. Ditmire *et al.*, Phys. Rev. A **53**, 3379 (1996).
[9] J. Zweiback, T. Ditmire, and M.D. Perry, Phys. Rev. A **59**, R3166 (1999).
[10] E. Parra *et al.*, Phys. Rev. E **62**, R5931 (2000).
[11] H.M. Milchberg, S.J. McNaught, and E. Parra, Phys. Rev. E **64**, 056402 (2001).
[12] K.Y. Kim, I. Alexeev, E. Parra, and H.M. Milchberg, Phys. Rev. Lett. **90**, 023401 (2003).
[13] V. Kumarappan, M. Krishnamurthy, and D. Mathur, Phys. Rev. Lett. **87**, 085005 (2001); Phys. Rev. A **66**, 033203 (2002).
[14] T. Ditmire, Phys. Rev. A **57**, R4094 (1998).
[15] K. Ishikawa and T. Blenski, Phys. Rev. A **62**, 063204 (2000).
[16] M. Eloy, R. Azambuja, J.T. Mendonca, and R. Bingham, Phys. Plasmas **8**, 1084 (2001).
[17] T. Tajima, Y. Kishimoto, and M.C. Downer, Phys. Plasmas **6**, 3759 (1999).
[18] I. Alexeev, T.M. Antonsen, K.Y. Kim, and H.M. Milchberg, Phys. Rev. Lett. **90**, 103402 (2003).
[19] The term Rayleigh scattering was used by several groups previously to describe the scattering of a laser pulse from nanoplasmas. However, as the nanoplasmas expand to form a uniform plasma, a transition from Rayleigh scattering to Thomson scattering takes place.
[20] S.-Y. Chen *et al.*, Phys. Rev. Lett. **80**, 2610 (1998).
[21] O.F. Hagena and W. Obert, J. Chem. Phys. **56**, 1793 (1972); O.F. Hagena, Rev. Sci. Instrum. **63**, 2374 (1992).
[22] J. Zweiback, T. Ditmire, and M.D. Perry, Opt. Express **6**, 236 (2000).
[23] J.W.G. Tisch, Phys. Rev. A **62**, 041802 (2000).